0022-3565/09/3301-283–293$20.00
THE JOURNAL OF PHARMACOLOGY AND EXPERIMENTAL THERAPEUTICS
JPET 330:283–293, 2009

Vol. 330, No. 1
150672/3482000
Printed in U.S.A.

The Intracellular II-III Loops of $Ca_v1.2$ and $Ca_v1.3$ Uncouple L-Type Voltage-Gated Ca^{2+} Channels from Glucagon-Like Peptide-1 Potentiation of Insulin Secretion in INS-1 Cells via Displacement from Lipid Rafts[S]

Sarah Melissa P. Jacobo, Marcy L. Guerra, Rachel E. Jarrard, Julie A. Przybyla, Guohong Liu, Val J. Watts, and Gregory H. Hockerman

Program in Biochemistry and Molecular Biology (S.M.P.J.), Purdue University Interdisciplinary Life Sciences Program (R.E.J.), and Department of Medicinal Chemistry and Molecular Pharmacology (M.L.G., J.A.P., G.L., V.J.W., G.H.H.), Purdue University, West Lafayette, Indiana

Received January 8, 2009; accepted April 6, 2009

ABSTRACT

L-type Ca^{2+} channels play a key role in the integration of physiological signals regulating insulin secretion that probably requires their localization to specific subdomains of the plasma membrane. We investigated the role of the intracellular II-III loop domains of the L-type channels $Ca_v1.2$ and 1.3 in coupling of Ca^{2+} influx with glucose-stimulated insulin secretion (GSIS) potentiated by the incretin hormone glucagon-like peptide (GLP)-1. In INS-1 cell lines expressing the $Ca_v1.2$/II-III or $Ca_v1.3$/II-III peptides, GLP-1 potentiation of GSIS was inhibited markedly, coincident with a decrease in GLP-1-stimulated cAMP accumulation and the redistribution of $Ca_v1.2$ and $Ca_v1.3$ out of lipid rafts. Neither the $Ca_v1.2$/II-III nor the $Ca_v1.3$/II-III peptide decreased L-type current density compared with untransfected INS-1 cells. GLP-1 potentiation of GSIS was restored by the L-type channel agonist 2,5-dimethyl-4-[2-(phenylmethyl)benzoyl]-1*H*-pyrrole-3-carboxylic acid methyl ester (FPL-64176). In contrast, potentiation of GSIS by 8-bromo-cAMP (8-Br-cAMP) was inhibited in $Ca_v1.2$/II-III but not $Ca_v1.3$/II-III cells. These differences may involve unique protein-protein interactions because the $Ca_v1.2$/II-III peptide, but not the $Ca_v1.3$/II-III peptide, immunoprecipitates Rab3-interacting molecule (RIM) 2 from INS-1 cell lysates. RIM2, and its binding partner Piccolo, localize to lipid rafts, and they may serve as anchors for $Ca_v1.2$ localization to lipid rafts in INS-1 cells. These findings suggest that the II-III interdomain loops of $Ca_v1.2$, and possibly $Ca_v1.3$, direct these channels to membrane microdomains in which the proteins that mediate potentiation of GSIS by GLP-1 and 8-Br-cAMP assemble.

The pancreatic β-cell transduces a chemical signal in the form of elevated extracellular glucose concentrations into electrical information, ultimately leading to the Ca^{2+}-dependent exocytosis of insulin from secretory vesicles. The prevailing model for glucose-stimulated insulin secretion (GSIS) from the pancreatic β-cell involves glucose entry via the transporter GLUT2, leading to the increase in [ATP] to [ADP] ratio and the closure of the ATP-sensitive potassium channel $Kir_{6.2}$/SUR1 (Rajan et al., 1990). The L-type voltage-gated Ca^{2+} channels (L-VGCCs) sense the consequent depolarization of the plasma membrane potential and conduct the influx of Ca^{2+} that is required for the docking and fusion of insulin secretory vesicles (Wollheim and Sharp, 1981). The cycle is reset upon the activation of K^+ channels that repolarize the membrane (Leung et al., 2007). Thus, membrane potential and intracellular Ca^{2+}

This work was supported by the National Institutes of Health National Institute of Diabetes and Digestive and Kidney Diseases [Grant R01-DK064736] (to G.H.H.); a Purdue Research Foundation award (to S.M.P.J. and G.H.H.); and a Showalter Trust Award (to G.H.H. and V.J.W.).

This work was in partial fulfillment of the requirements for Jacobo SMP (2008) Dichotomy of $Ca_v1.2$ and $Ca_v1.3$ L-type Ca^{2+} channel function and modulation in GLP-1-mediated insulin exocytosis and ERK1/2 activation in pancreatic beta cells. Ph.D. thesis, Purdue University, West Lafayette, Indiana.

Article, publication date, and citation information can be found at http://jpet.aspetjournals.org.

doi:10.1124/jpet.109.150672.

[S] The online version of this article (available at http://jpet.aspetjournals.org) contains supplemental material.

ABBREVIATIONS: GSIS, glucose-stimulated insulin secretion; L-VGCC, L-type voltage-gated Ca^{2+} channel; 8-Br-cAMP, 8-bromo-cAMP; EPAC2, exchange protein activated by cAMP2; RIM, Rab3-interacting molecule; GLP-1R, glucagon-like peptide-1 receptor; GLP, glucagon-like peptide; PBS, phosphate-buffered saline; KRBH Krebs-Ringer bicarbonate HEPES; BSA, bovine serum albumin; BCA, bicinchoninic acid; GFP, green fluorescent protein; PAGE, polyacrylamide gel electrophoresis; PBST, phosphate-buffered saline containing 0.1% Tween 20; MES, 2-(*N*-morpholino)ethanesulfonic acid; I_{Ba}, barium current; FPL-64176, 2,5-dimethyl-4-[2-(phenylmethyl)benzoyl]-1*H*-pyrrole-3-carboxylic acid methyl ester; mβCD, methyl-β-cyclodextrin.

concentration undergo coordinate oscillations in β-cells in the presence of glucose (Bergsten, 2002).

We have shown previously that the neuroendocrine-specific channel $Ca_v1.3$ is preferentially coupled to GSIS (Liu et al., 2003) and glucose-stimulated Ca^{2+} oscillations (Liu et al., 2004) in the rat insulinoma cell line INS-1. In contrast, we reported previously that both $Ca_v1.2$ and $Ca_v1.3$ can mediate GSIS potentiated by 8-Br-cAMP, but that only $Ca_v1.2$ can mediate potentiation of GSIS by activation of exchange protein activated by cAMP2 (EPAC2) independently of protein kinase A activation (Liu et al., 2006). These data suggest that these secretagogue-mediated events share parallel and overlapping signaling effectors that, at the same time, require different sources of Ca^{2+}. However, it is clear that L-VGCCs are key effectors in these distinct paradigms of exocytosis.

The structural and functional features of $Ca_v1.2$ and $Ca_v1.3$ that specify their distinct roles in glucose-mediated events in pancreatic β-cells cells remain unclear. The $Ca_v1.2$ and $Ca_v1.3$ α_1 pore subunits are composed of four highly conserved hexahelical transmembrane domains; however, the cytoplasmic loops that connect each domain show higher sequence divergence (Catterall, 1995). In particular, the intracellular linker between domains II and III of $Ca_v1.2$ and $Ca_v1.3$ share only ~40% amino acid sequence identity. In the β-cell, experiments with peptides corresponding to the $Ca_v1.2$ II-III interdomain loop have suggested that $Ca_v1.2$ interacts with members of the insulin secretory machinery, including synaptotagmin, syntaxin (Wiser et al., 1999), and soluble *N*-ethylmaleimide-sensitive factor attachment protein-25 (Ji et al., 2002). In addition, the multifunctional scaffolding protein Rab3-interacting molecule (RIM) 2 and its interacting partner Piccolo are proposed to bind the II-III loop of $Ca_v1.2$ (Shibasaki et al., 2004). The Ca^{2+}-dependent heterodimer formed by RIM2 and Piccolo has also been shown to interact with EPAC2, a guanine nucleotide exchange factor that also interacts with the secretory vesicle-specific Rab3 GTPase (Shibasaki et al., 2004). The $Ca_v1.3$ channel is functionally modulated by syntaxin 1 and vesicle-associated membrane protein (Song et al., 2003) and is coimmunoprecipitated by antibodies to syntaxin 1 from mouse pancreatic islets (Yang et al., 1999). However, the role of the II-III interdomain loop of $Ca_v1.3$ in channel localization or protein-protein interactions is unknown.

The assembly of proteins that regulate insulin exocytosis from pancreatic β-cells may center on cholesterol and glycosphingolipid-rich "lipid raft" domains in the plasma membrane that promote colocalization of functionally related proteins. Caveolae are a subset of lipid raft domains (Cohen et al., 2004). In pancreatic β-cells, in which the caveolae-resident proteins caveolin-1 and -2 are present (Xia et al., 2004), proteins of the macromolecular exocytosis complex, such as soluble *N*-ethylmaleimide-sensitive factor attachment protein-25, syntaxin-1A, vesicle-associated membrane protein 2, $K_v2.1$, and $Ca_v1.2$ colocalize with caveolin-1 in lipid raft domains in the mouse β-cell line MIN6 (Xia et al., 2004). In addition, localization of the glucagon-like peptide-1 receptor (GLP-1R) to caveolae is essential for GLP-1R trafficking to the plasma membrane and GLP-1 stimulation of extracellular signal-regulated kinase 1/2 phosphorylation in MIN6 β-cells (Syme et al., 2006).

In the present study, we report that overexpression of the II-III loop of $Ca_v1.2$ or $Ca_v1.3$ differentially inhibits GLP-1 and 8-Br-cAMP potentiation of GSIS, coincident with a shift of the corresponding endogenous channels out of the Triton X-100-insoluble lipid raft fractions of a discontinuous sucrose gradient. Furthermore, we demonstrate that the $Ca_v1.2$ II-III loop, but not the $Ca_v1.3$ II-III loop, coimmunoprecipitates the active zone scaffolding protein RIM2 from INS-1 cells. Taken together, our results suggest that the II-III interdomain loops of $Ca_v1.2$ and $Ca_v1.3$ target their respective channels to membrane microdomains via protein interaction networks that are critical for efficient potentiation of glucose-dependent events by GLP-1 receptor activation in pancreatic β-cells.

Materials and Methods

Reagents. All reagents used in this study, unless otherwise stated, were obtained from Sigma-Aldrich (St. Louis, MO). The truncated and amidated human peptide $GLP\text{-}1^{7\text{-}36NH2}$, simply denoted as GLP-1, was used for all insulin secretion assays. The membrane-soluble, phosphodiesterase-resistant cAMP nucleotide analog 8-Br-cAMP was obtained from Calbiochem (San Diego, CA).

Plasmids and Stable Cell Line Construction. The cDNAs that encode the cytoplasmic II-III interdomain loop of $Ca_v1.2$ (amino acids 758–903) or $Ca_v1.3$ (amino acids 752–885) fused to enhanced GFP were constructed in the pEGFP-N1 vector (Clontech, Mountain View, CA) as described previously (Liu et al., 2003). Clonal INS-1 cell lines stably expressing these constructs ($Ca_v1.2$/II-III cells and $Ca_v1.3$/II-III cells) were selected and characterized as described previously (Liu et al., 2003).

Cell Culture. INS-1 Cells (a generous gift from Dr. Min Li, Tulane University, New Orleans, LA) were maintained in a humidified atmosphere of 37°C and 5% CO_2 in RPMI 1640 medium, pH 7.35, that contained 11.2 mM glucose, 10 mM glutamine, 48 mM $NaHCO_3$, 20 mM HEPES, and 50 μM β-mercaptoethanol as specified previously (Asfari et al., 1992). The culture media were supplemented with, 100 U/ml penicillin, 100 μg/ml streptomycin (Invitrogen, Carlsbad, CA), 1 mM sodium pyruvate, and 10% (v/v) fetal bovine serum (HyClone Laboratories, Logan, UT).

Insulin Secretion Assays. INS-1 cells in 12-well plates were washed twice with isotonic PBS and preincubated with modified Krebs-Ringer buffer [KRBH; 115 mM NaCl, 5 mM KCl, 1 mM $MgCl_2$, 2.5 mM $CaCl_2$, 24 mM $NaHCO_3$, 25 mM HEPES, 0.05% bovine serum albumin (BSA), pH 7.3; 295 mOsM] for 30 min at 37°C, 5% CO_2. The preincubation buffer was removed and replaced with KRBH buffer containing the stimuli. After the incubation of cells for 30 min at 37°C, 5% CO_2, the conditioned buffer was removed and stored at −20°C for assay of secreted insulin content. The whole-cell insulin content was extracted by incubation of cells in HCl-ethanol buffer [3% HCl, 16% ethanol, and 57% H_2O (v/v)] for 12 to 16 h at 4°C. On the day of the assay, the whole-cell insulin content was diluted 10-fold with glycine-NaOH-BSA buffer. Insulin content in the secreted and the whole-cell fractions was assayed by the Rat Insulin High Range enzyme-linked immunosorbent assay kit (ALPCO, Salem, NH), according to the manufacturer's instructions. Where indicated, insulin secretion was normalized to total cellular protein. Protein was quantified using the BCA assay (Pierce Chemical, Rockford, IL).

cAMP Accumulation Assay. Two days before the assay, cells were seeded in 24-well tissue culture plates to achieve ~90% confluence. On the day of the assay, cells were placed on ice while GLP-1 or forskolin in KRBH buffer (supplemented with 500 μM isobutylmethylxanthine and 0.5% BSA) was added. Drug treatments were performed for 15 min in a 37°C water bath. The assay buffer was decanted to terminate the stimulation, and cells were lysed by adding 200 μl of 3% trichloroacetic acid on ice. Plates were stored at 4°C for at least 1 h before cAMP quantification by competitive radioligand binding assay as described previously (Cumbay and Watts,

2001). Results were normalized over total protein content and expressed as percentage of maximal forskolin stimulation.

Immunoprecipitation Assays. Wild-type INS-1 cells transfected with GFP (INS-1/GFP), $Ca_v1.2$/II-III/GFP cells, and $Ca_v1.3$/II-III/GFP cells were lysed with lysis buffer [20 mM Na_2HPO_4, 150 mM NaCl, 0.1% Triton X-100, and 60 mM 1-*O*-*n*-octyl-β-D-glucopyranoside (*n*-ocylglucoside), pH 7.4] supplemented with protease inhibitors for 30 min on ice. The supernatant was clarified twice by centrifugation. Protein concentrations were determined using the BCA assay (Pierce Chemical). Fifty microliters of a slurry containing an affinity-purified GFP antibody covalently coupled to 4% agarose beads (Vector Laboratories, Burlingame, CA) was incubated overnight with a 0.5% BSA solution made with lysis buffer (without *n*-ocylglucoside) with gentle shaking at 4°C. Samples were then centrifuged at 5000*g* for 1 min to remove the BSA solution. The beads were washed three times with lysis buffer (without *n*-octylglucoside) to remove residual BSA. The beads were then incubated with 500 μg of protein from INS-1/GFP, $Ca_v1.2$/II-III/GFP, or $Ca_v1.3$/II-III/GFP cell lysates overnight with gentle shaking at 4°C. Samples were then centrifuged at 5000*g* for 1 min, and the supernatant was collected ("unbound"). The beads were then washed with 200 μl of wash buffer (20 mM Na_2HPO_4, 1 M NaCl, and 0.1% Triton X-100, pH 7.4) five times. Only the final wash was collected ("wash"). Proteins were eluted from the beads using elution buffer (100 mM Tris, 1 M glycine, 200 mM SDS, and 1 mM dithiothreitol) with heating at 80°C. The samples were centrifuged at 5000*g* for 1 min, and the supernatant was collected ("eluate"). Proteins in the cell lysates, wash, and eluate samples from the pull-down were separated by SDS-polyacrylamide gel electrophoresis (PAGE) and transferred to polyvinylidene difluoride membranes. Fifty micrograms of protein from cell lysates and 50 μl of the pull-down assay samples were loaded. Membranes were blocked with 5% nonfat milk in PBS containing 0.1% Tween 20 (PBST) for 2 h at room temperature. Membranes were incubated with primary antibodies overnight at 4°C: RIM2, 1:500 (Synaptic Systems); GFP, 1:1000 (Santa Cruz Biotechnology, Inc.). The membranes were then washed with PBST and incubated with horseradish peroxidase-conjugated secondary antibodies for 1 h at room temperature. The membranes were washed with PBST, incubated in enhanced chemiluminescence reagent for 1 min, and exposed to film (BioMax XAR film; Eastman Kodak, Rochester, NY).

Sucrose Density Gradient Ultracentrifugation and Isolation of Triton X-100-Insoluble Membrane Fractions. INS-1 cells were washed twice with isotonic PBS lysed in 2.5 ml of ice-cold MBS buffer (25 mM MES, 150 mM NaCl, and 1% Triton X-100, pH 6.5) by Dounce homogenization. Cell lysates were transferred to Ultra-Clear centrifuge tubes (Beckman Coulter, Fullerton, CA) and diluted with an equal volume of MBS buffer containing 90% sucrose. The resulting 45% sucrose fraction was successively layered with MBS buffer containing 30% sucrose (4 ml) and 5% sucrose (2 ml). All buffers were supplemented with protease inhibitors. The discontinuous sucrose gradients were centrifuged at 40,000 rpm for 18 h at 4°C in an Optima L/LE ultracentrifuge (Beckman Coulter) using an SW41Ti rotor. Aliquots (1 ml) were carefully taken from the top layer and assayed for protein concentration using the BCA assay. The first six aliquots (fractions 1–6) were further concentrated by centrifugation at 5000*g* in Centricon YM-10 filtration tubes (Millipore, Billerica, MA) to 1/10 the original volume. For each sample, 20 to 25 μg of total protein per well was loaded with Laemmli buffer (0.01% bromphenol blue, 0.1 M dithiothreitol, 10% glycerol, and 10 mM Tris, pH 6.8) in 8, 10, or 12% Tris-glycine gels. Proteins were electrotransferred to polyvinylidene difluoride membranes (Bio-Rad Laboratories, Hercules, CA) and incubated in blocking buffer (5% nonfat dry milk in PBST) for 3 h at room temperature. Membranes were incubated with primary antibodies (1:500 dilution) overnight at 4°C and washed with phosphate-buffered saline at room temperature. Specific immunoreactivity was detected with horseradish peroxidase-conjugated secondary antibodies (Bio-Rad Laboratories) after enhanced chemiluminescence developing. Primary antibodies generated against portions of the II-III interdomain loop of $Ca_v1.2$ (amino acids 848–865) or $Ca_v1.3$ (amino acids 859–875) were obtained from Millipore Bioscience Research Reagents (Temecula, CA). The caveolin-1 antibody was obtained from Santa Cruz Biotechnology, Inc. (Santa Cruz, CA). The Piccolo antibody was a generous gift from Dr. Craig Garner (Stanford University, Stanford, CA). All immunoblots are representative of at least three repeats.

Electrophysiology. INS-1 cells were seeded in plastic 35-mm tissue culture dishes (Nalge Nunc International, Rochester, NY) to 40% confluence. Whole-cell barium currents (I_{Ba}) were recorded at room temperature using an Axopatch 200B amplifier (Molecular Devices, Sunnyvale, CA) and filtered at 1 kHz (six-pole Bessel filter, 4-pole Bessel filter). Electrodes were pulled from borosilicate glass (VWR, West Chester, PA) and fire-polished to achieve resistance values of 2 to 6 MΩ. Data were acquired after applying 500-ms test potentials from −50 to +60 mV, at 10-mV increments, with pClamp 8 software (Molecular Devices). The L-VGCC antagonists nifedipine (Sigma/RBI, Natick, MA) and diltiazem (Sigma-Aldrich) were applied to the recording chamber in bath saline at the rate of 0.5 ml/min. The bath solution contained 150 mM Tris, 10 mM $BaCl_2$, and 4 mM $MgCl_2$. The intracellular solution contained 130 mM *N*-methyl-D-glucamine, 10 EGTA, 60 mM HEPES, 2 mM ATP, and 1 mM $MgCl_2$. The pH of both solutions was adjusted to 7.3 with methanesulfonic acid, and the osmotic pressure was corrected to 290 to 300 mOsM. Total current density (pA/pF) is expressed as mean ± S.E.M.

Data Analysis. Data were analyzed using SigmaPlot 11.0 for Windows (Systat Software, Inc., San Jose, CA) or Prism 5 for Macintosh (GraphPad Software Inc., San Diego, CA). Data are represented as mean values of at least three trials ± S.E.M. Statistical analyses of data sets were performed using one-way analysis of variance with the Holm-Sidak post hoc comparison with SigmaPlot 11.0.

Results

In the presence of 7.5 mM glucose, stimulation of the INS-1 rat insulinoma cell line with 50 nM GLP-1 results in robust potentiation of GSIS, which is blocked substantially by 10 μM nifedipine, an L-VGCC antagonist (Fig. 1A). To examine the role of the α_1 II-III interdomain peptide of $Ca_v1.2$ and $Ca_v1.3$ in GLP-1-potentiated insulin secretion mediated by these channels, we stably expressed enhanced GFP-tagged peptides corresponding to the full-length II-III interdomain peptides of $Ca_v1.2$ (amino acids 758–903) and $Ca_v1.3$ (amino acids 752–885) (Fig. 1B) in INS-1 cells. We performed insulin secretion assays in the presence of 50 nM GLP-1 and varying glucose concentrations that mimic pre- and postprandial blood glucose levels in untransfected INS-1 cells, and INS-1 cells overexpressing either the $Ca_v1.2$/II-III or $Ca_v1.3$/II-III peptides. Marked potentiation of GSIS by GLP-1 was observed in untransfected INS-1 cells at all glucose concentrations tested above 5 mM (Fig. 1C). In contrast to GLP-1 potentiation of GSIS from INS-1 cells, GLP-1 potentiation of GSIS in $Ca_v1.2$/II-III and $Ca_v1.3$/II-III cells was essentially absent over a physiologically relevant range of glucose concentrations (5–25 mM glucose; Fig. 1C). This attenuation of insulin secretion was not accompanied by a change in the cellular insulin content (data not shown). Given the critical role of L-VGCC activity in GSIS, we next examined the ability of the L-type channel activator FPL-64176 to rescue GSIS in $Ca_v1.2$/II-III and $Ca_v1.3$/II-III cells. Indeed, robust recovery of GLP-1 potentiation of GSIS was observed in the presence of 50 μM FPL-64176 and was completely blocked by the L-type channel antagonist diltiazem (Fig. 1D). Thus, it seems that augmentation of Ca^{2+} influx via endogenous L-type channels with FPL-64176 is sufficient to recover

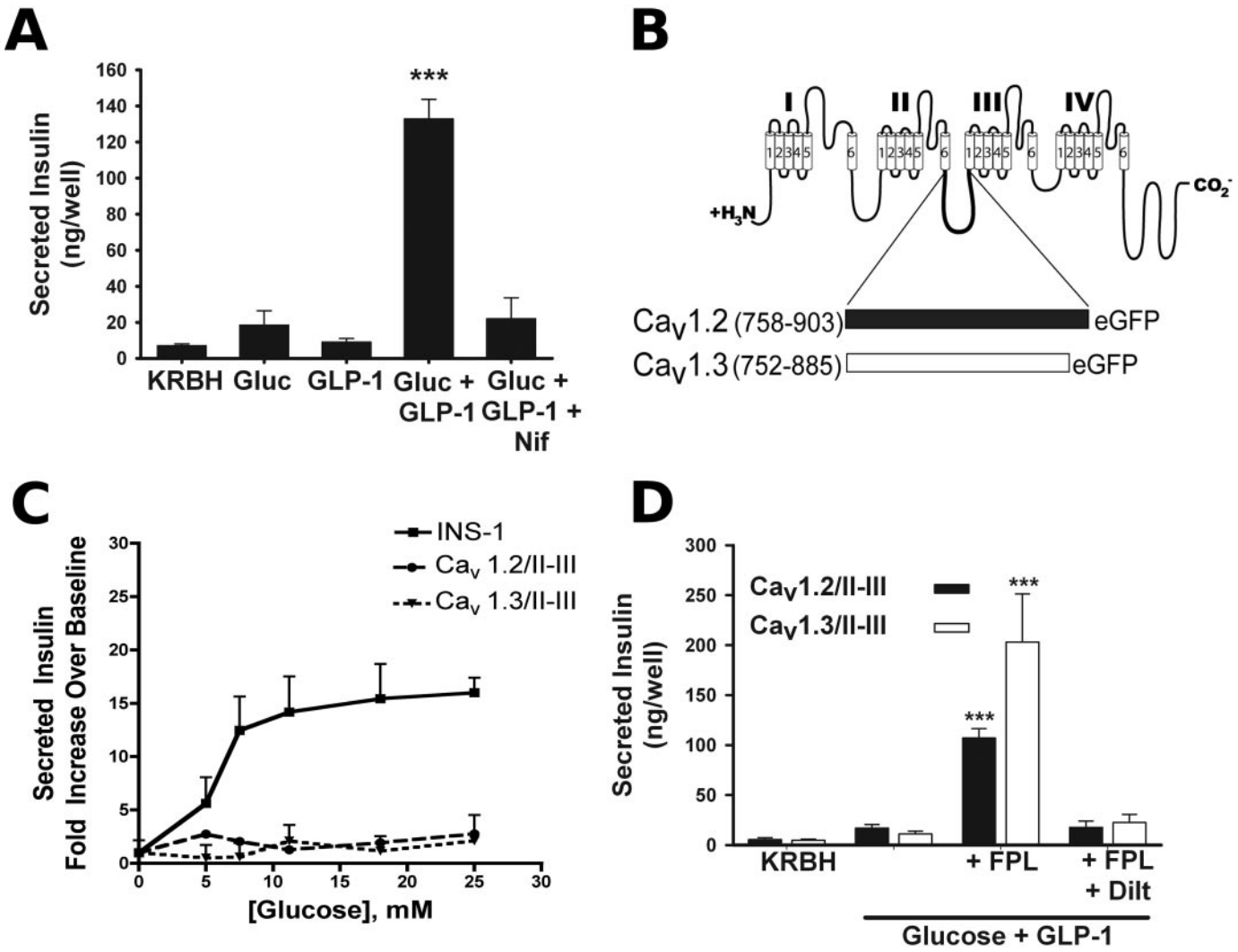

Fig. 1. Overexpression of peptides corresponding to the full-length α_1 II-III interdomain loops of $Ca_v1.2$ and $Ca_v1.3$ abrogates potentiation of glucose-stimulated insulin secretion by GLP-1. A, 50 nM GLP-1 robustly potentiates 7.5 mM glucose-stimulated insulin secretion in INS-1 cells. This amplified response is sensitive to the L-VGCC blocker nifedipine (10 μM). ***, $P < 0.001$ compared with all other conditions ($n = 3–10$; $F = 47.5$). B, diagram of the II-III interdomain linker peptide of the L-VGCC subunits $Ca_v1.2$ and $Ca_v1.3$ fused to GFP that were stably transfected in INS-1 cells. Numbers indicate amino acids included in the fusions from $Ca_v1.2$ (M67515.1, GI: 2065770) and $Ca_v1.3$ (NM_001128840, GI: 192807299). C, in INS cells, 50 nM GLP-1 amplifies insulin secretion in response to a physiological range of glucose concentrations (5–25 mM). This glucose concentration dependence of insulin release is abolished upon overexpression of the $Ca_v1.2$/II-III or the $Ca_v1.3$/II-III peptide. Secretion is expressed as -fold increase over KRBH. D, L-type channel "agonist" FPL-64176 (50 μM) rescues GLP-1 potentiation of GSIS in INS-1 cells overexpressing the $Ca_v1.2$/II-III or $Ca_v1.3$/II-III peptides. This recovery of secretion by FPL-64176 is completely blocked by 500 μM diltiazem. ***, $P < 0.001$ compared with all other conditions within the same cell line ($Ca_v1.2$/II-III: $n = 7–13$, $F = 51.5$; and $Ca_v1.3$/II-III: $n = 5–13$, $F = 17.4$).

GLP-1 potentiation of GSIS in $Ca_v1.2$/II-III and $Ca_v1.3$/II-III cells.

Given the central role of L-VGCC in mediating insulin secretion, the lack of GLP-1-potentiated GSIS in the $Ca_v1.2$/II-III and $Ca_v1.3$/II-III cells could be explained by alterations in the endogenous L-VGCC activity. Therefore, we measured the whole-cell Ba^{2+} current in $Ca_v1.2$/II-III and $Ca_v1.3$/II-III cells and compared the voltage dependence of the current, the total current density, and the fraction of the current blocked by 10 μM nifedipine with that measured in untransfected INS-1 cells. The peak current-voltage curves for all three cell lines from a holding potential of −70 mV in the presence and absence of 10 μM nifedipine are shown in Fig. 2, A to C. The threshold of activation and reversal potential were similar across the three cell lines either in the absence or presence of nifedipine. Using the peak tail current-voltage curve from these experiments, we found that $V_{1/2act}$ in untransfected INS-1 cells, $Ca_v1.2$/II-III cells, and $Ca_v1.3$/II-III cells was not significantly different (INS-1 = −17.9 ± 1.6 mV, $n = 8$; $Ca_v1.2$/II-III = −14.9 ± 3.4 mV, $n = 12$; and $Ca_v1.3$/II-III = −17.3 ± 1.2 mV, $n = 12$) (Fig. 2D). Likewise, the $V_{1/2act}$ was not significantly different in the presence or absence of nifedipine for all three cell lines (data not shown). The mean whole-cell I_{Ba} density from untransfected INS-1 cells was not significantly different from that measured in $Ca_v1.3$/II-III cells (Fig. 2E). However, $Ca_v1.2$/II-III cells exhibited voltage-gated I_{Ba} density significantly greater than that of either untransfected INS-1 cells or $Ca_v1.3$/II-III cells (Fig. 2E). The fraction of the whole-cell I_{Ba} contributed by L-VGCC in untransfected INS-1 cells, $Ca_v1.2$/II-III cells, and $Ca_v1.3$/II-III cells was estimated by measuring the fraction of whole-cell current blocked by 10 μM nifedipine. No statistically significant difference was detected in the fraction of current blocked by 10 μM nifedipine among these three cell

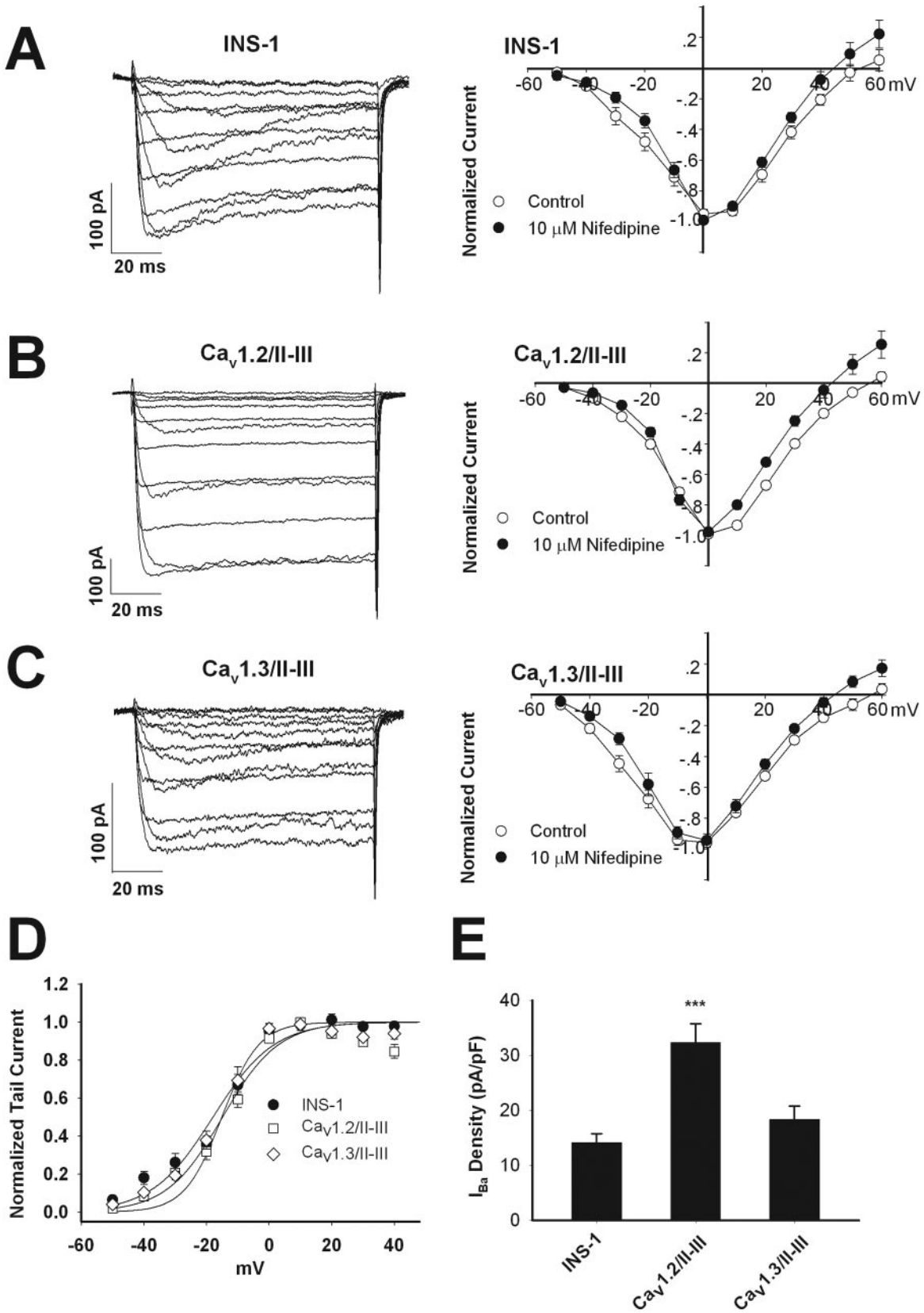

Fig. 2. Endogenous voltage-gated Ca^{2+} channel activity is intact in INS-1 cells overexpressing $Ca_v1.2$/II-III or $Ca_v1.3$/II-III peptides. A to C, current-voltage relationship curves of I_{Ba} measured using whole-cell voltage clamp. Currents were elicited by 100-ms depolarizations from −50 to +60 mV in 10-mV increments, from a holding potential of −70 mV, in the absence (control, ○) or presence of 10 μM nifedipine (●). INS-1 cells (n = 10), $Ca_v1.2$/II-III cells (n = 10), and $Ca_v1.3$/II-III cells (n = 8). D, peak tail currents recorded upon repolarization to −70 mV after a 100-ms depolarization to the indicated prepulse voltage were normalized and plotted against prepulse voltage. $V_{1/2act}$ values were determined by fitting the data to the equation $I/I_{max} = 1/(1 + \exp[-(V - V_{1/2})/K])$, where V is the prepulse potential in millivolts and $V_{1/2}$ is the prepulse potential at which tail current amplitude is half-maximal. E, whole-cell I_{Ba} density (pA/pF) measured at 0 mV from a holding potential of −70 mV. The difference in total whole-cell current density for $Ca_v1.2$/II-III cells compared with INS-1 cells and $Ca_v1.3$/II-III cells is statistically significant. ***, $P < 0.001$ (n = 13–15, F = 13.9).

lines (Fig. 3). Thus, the profound inhibition of GLP-1 potentiation of GSIS upon overexpression of the $Ca_v1.2$/II-III or $Ca_v1.3$/II-III peptides cannot be explained by a decrease in L-type current density or in a change in voltage dependence of Ca^{2+} channel activation.

A potential explanation for the loss of GLP-1 potentiation of GSIS in $Ca_v1.2$/II-III and $Ca_v1.3$/II-III cells might be the disruption of GLP-1 stimulation of cAMP accumulation in these cell lines. Therefore, we assayed the GLP-1-stimulated accumulation of cAMP in untransfected INS-1 cells and the $Ca_v1.2$/II-III and $Ca_v1.3$/II-III cell lines. As shown in Fig. 4A, 10 and 100 nM GLP-1 significantly increased cAMP levels above baseline. In both concentrations tested, cAMP accumulation in response to GLP-1 in both $Ca_v1.2$/II-III and $Ca_v1.3$/II-III cells was reduced ~50% compared with control INS-1 cells. Subsequent experiments revealed that addition of glucose (7.5 mM) did not alter GLP-1-stimulated cAMP accumulation in any of the cell lines (Fig. 4B). Furthermore, the addition of 50 μM FPL-64176 with or without 7.5 mM glucose did not significantly increase cAMP accumulation stimulated by 100 nM GLP-1 in any of the cell lines (Supplemental Fig. 1). To determine whether attenuation of cAMP accumulation in $Ca_v1.2$/II-III or $Ca_v1.3$/II-III cells occurs only in response to GLP-1, we measured cAMP levels in response to the receptor-independent activator of adenylyl cyclase, forskolin. In INS-1 cells, forskolin (1–300 μM) dose-dependently stimulated cAMP accumulation in a manner that was not significantly different from $Ca_v1.2$/II-III or $Ca_v1.3$/II-III cells and was not different in the presence of 7.5 mM glucose (Supplemental Fig. 1). Thus, the inability of GLP-1 to potentiate GSIS in either $Ca_v1.2$/II-III or $Ca_v1.3$/II-III cells can be at least partially ascribed to a decrease in GLP-1-stimulated cAMP accumulation. Moreover, the rescue of GLP-1 potentiation of GSIS in $Ca_v1.2$/II-III and $Ca_v1.3$/II-III cells by FPL-64176 does not seem to involve an increase in cAMP accumulation. Because GLP-1 stimulation of cAMP accumulation was attenuated in $Ca_v1.2$/II-III and $Ca_v1.3$/II-III cells, we examined the ability of 8-Br-cAMP to potentiate GSIS in these cells as well as in untransfected INS-1 cells. The combination of 7.5 mM glucose and 1 mM 8-Br-cAMP potentiated GSIS in both untransfected INS-1 cells and $Ca_v1.3$/II-III cells to a similar extent (Fig. 4C). However, in $Ca_v1.2$/II-III cells, 1 mM 8-Br-cAMP did not significantly potentiate GSIS. Thus, overexpression of the $Ca_v1.2$/ II-III loop, but not the $Ca_v1.3$/II-III loop, results in the inhibition of cAMP-potentiated GSIS.

Given that overexpression of the $Ca_v1.2$ and $Ca_v1.3$ II-III loops has profound but differential effects on GLP-1 and 8-Br-cAMP potentiation of GSIS, we considered the possibility that localization of the endogenous L-VGCC was disrupted in $Ca_v1.2$/II-III and $Ca_v1.3$/II-III cells compared with untransfected INS-1 cells. $Ca_v1.2$ from cardiovascular tissue (Tsujikawa et al., 2008) as well as insulin-secreting cells (Xia et al., 2004) is reported to localize to low-density lipid raft fractions of sucrose gradients in a manner that is disrupted by cholesterol-depleting agents. Therefore, untransfected INS-1 cells, $Ca_v1.2$/II-III cells, and $Ca_v1.3$/II-III cells were lysed in ice-cold buffer containing Triton X-100, and the lysates were separated by centrifugation across a discontinuous 5/30/45% sucrose density gradient (Xia et al., 2004). This technique allows the isolation of lipid raft fractions from the rest of the membrane components; cytosolic and Triton X-100-soluble membrane proteins remain in the 45% layer, and the buoyant Triton X-100-insoluble lipid rafts partition to the interface of the 5 and 30% gradients. Western blot analysis demonstrates that in untransfected INS-1 cells, $Ca_v1.2$ and $Ca_v1.3$ cosediment in the low-density, Triton X-100-insoluble fractions, along with caveolin-1 (Fig. 5, A–C). Remarkably, in $Ca_v1.2$/II-III cells, we found a shift in the distribution of the endogenous α_1 pore subunit $Ca_v1.2$, from Triton X-100-insoluble to Triton X-100-soluble fractions that was not observed in $Ca_v1.3$/II-III cells (Fig. 5A). In $Ca_v1.3$/II-III cells, a similar shift of the endogenous $Ca_v1.3$ channels from Triton X-100-insoluble to Triton X-100-soluble fractions was observed, but this shift was not observed in $Ca_v1.2$/II-III cells (Fig. 5B). In both $Ca_v1.2$/II-III and $Ca_v1.3$/II-III cells, caveolin-1 distribution was not different from untransfected INS-1 cells (Fig. 5C).

Because it is reported that disruption of lipid rafts with the cholesterol binding agent methyl-β-cyclodextrin (mβCD) en-

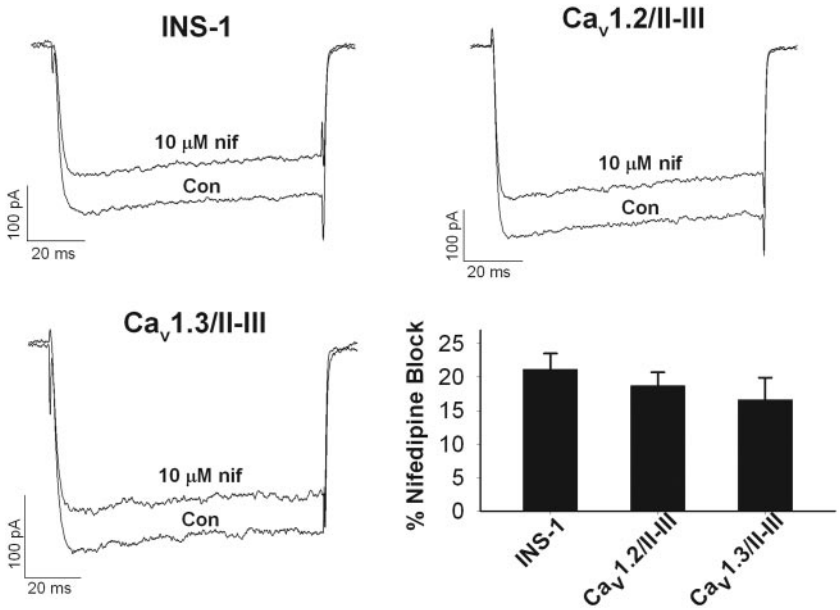

Fig. 3. Overexpression of the $Ca_v1.2$/I-III and $Ca_v1.3$/II-III loop peptides does not affect the percentage of whole-cell L-type Ca^{2+} channels in INS-1 cells. Example whole-cell I_{Ba} traces were recorded from INS-1, $Ca_v1.2$/II-III, and $Ca_v1.3$/II-III cells, respectively, showing baseline current (con) and current after coming to equilibrium in the presence of 10 μM nifedipine (nif) applied in the extracellular solution. Cells were held at −70 mV and current elicited by pulsing to +10 mV for 100 ms. Percentage of the whole-cell I_{Ba} blocked by 10 μM nifedipine (ns, one-way analysis of variance, F = 0.78) is shown.

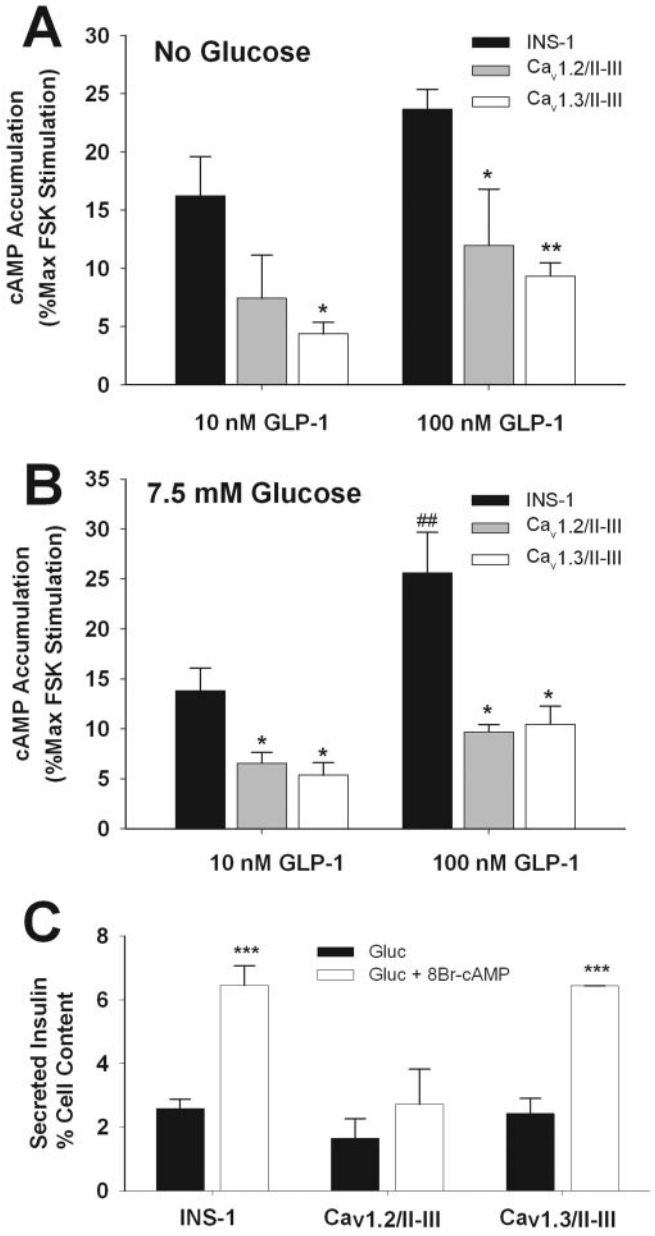

Fig. 4. Overexpression of the $Ca_v1.2$/II-III or $Ca_v1.3$/II-III peptide reduces GLP-1-stimulated cAMP accumulation in INS-1 cells. A, in $Ca_v1.2$/II-III or $Ca_v1.3$/II-III cells, GLP-1-stimulated cAMP accumulation is reduced compared with control INS-1 cells. Expressed as percentage of cAMP accumulation stimulated with 300 μM forskolin. *, $P < 0.05$; **, $P < 0.01$ compared with INS-1 cells ($n = 5$, $F = 5.4$). B, addition of glucose (7.5 mM) did not alter cAMP accumulation in INS-1, $Ca_v1.2$/II-III, or $Ca_v1.3$/II-III cells. *, $P < 0.05$ compared with INS-1 cells; ##, $P < 0.01$ compared with 10 nM GLP-1 in INS-1 cells ($n = 3$, $F = 11.5$). For all cell lines, the forskolin dose-response curves with or without glucose are not significantly different (see Supplemental Fig. 1). C, overexpression of the $Ca_v1.2$/II-III loop, but not the $Ca_v1.3$/II-III loop, inhibits potentiation of 7.5 mM GSIS by 1 mM 8-Br-cAMP. Secreted insulin is expressed as percentage of cell content. ***, $P < 0.001$ relative to glucose alone ($n = 3$, $F = 12.1$).

hances GSIS in HIT-t15 cells (Xia et al., 2004), we tested the effect of mβCD on GSIS and the potentiation of GSIS by 50 nM GLP-1 in INS-1 cells. We found that pretreatment of INS-1 cells with 10 mM mβCD does not inhibit GLP-1 potentiation of 7.5 mM GSIS but significantly enhances 7.5 mM GSIS, as reported previously (Fig. 6A). Furthermore, we found that treatment of INS-1 cells with mβCD did not grossly affect the distribution of caveolin 1 to lipid raft fractions of sucrose gradients (Fig. 6B), consistent with the previous observations in HIT-t15 cells. Thus, overexpression of the $Ca_v1.2$/II-III and $Ca_v1.3$/II-III loops has a distinct effect on the potentiation of GSIS by GLP-1 in INS-1 cells compared with that of pretreatment with mβCD. In addition, neither overexpression of the II-III loop nor treatment with mβCD displaces caveolin 1 from lipid rafts in INS-1 cells.

Given that the II-III interdomain peptides of $Ca_v1.2$ and $Ca_v1.3$ seem to be major determinants in the localization of the respective channels to lipid rafts, we examined the possibility that specific protein-protein interactions may mediate this localization. We performed pull-down experiments on cell lysates from $Ca_v1.2$/II-III and $Ca_v1.3$/II-III cells, using anti-GFP antibodies covalently coupled to agarose. Because the scaffold protein RIM2 binds directly to the $Ca_v1.2$/II-III loop using an in vitro binding experiment (Shibasaki et al., 2004), we assayed the immunoprecipitates from $Ca_v1.2$/II-III cells and $Ca_v1.3$/II-III cells for the presence of RIM2. As shown in Fig. 7A, endogenous, full-length RIM2 was coimmunoprecipitated with the $Ca_v1.2$/II-III/GFP fusion from $Ca_v1.2$/II-III cell lysates and specifically eluted (lane E) after extensive washing, but not with the $Ca_v1.3$/II-III/GFP fusion from $Ca_v1.3$/II-III cells, or with GFP transiently expressed in INS-1 cells. In these experiments, we consistently observe a slight decrease in mobility of the $Ca_v1.3$/II-III-GFP fusion on SDS-PAGE after elution from the affinity matrix, whereas the $Ca_v1.2$/II-III loop mobility is unchanged. This change in mobility of the $Ca_v1.3$/II-III-GFP fusion is observed in Western blots using both the GFP antibody (Fig. 7A) and the $Ca_v1.3$/II-III loop antibody (data not shown). Because the $Ca_v1.3$/II-III loop contains two Cys residues but the $Ca_v1.2$/II-III loop contains only one residue, the most likely explanation for this anomaly is that heating the samples to 80°C in the presence of 1 mM dithiothreitol completely reduces a disulfide bond within the $Ca_v1.3$/II-III loop that is not present in the $Ca_v1.2$/II-III loop. Indeed, reduction of disulfide bonds is well known to decrease the electrophoretic mobility of proteins on SDS-PAGE (Griffith, 1972).

Because $Ca_v1.2$ resides in lipid raft fractions of the plasma membrane in β-cells (Xia et al., 2004; Fig. 5) and overexpression of the $Ca_v1.2$/II-III shifts $Ca_v1.2$ out of lipid rafts, we examined whether either of the proteins shown to coimmunoprecipitate with the $Ca_v1.2$/II-III loop were lipid raft residents. We found that the scaffold proteins RIM2 and Piccolo both colocalize extensively with the lipid raft fractions of a discontinuous sucrose gradient (Fig. 7, B and C) in untransfected INS-1 cells, and this localization was not different in $Ca_v1.2$/II-III cells. Thus, the putative interaction partner of the $Ca_v1.2$ II-III loop, RIM2, and its binding partner, Piccolo, are present in lipid rafts, and are not displaced by overexpression of the interdomain II-III loop of $Ca_v1.2$.

Discussion

Expression of $Ca_v1.2$ and 1.3 II-III Loops Displaces the Respective Channel from Lipid Rafts in INS-1 Cells. The key event leading to the uncoupling of the endogenous L-VGCC from GLP-1 potentiation of GSIS is the displacement of the $Ca_v1.2$ and $Ca_v1.3$ channels from lipid rafts by their respective II-III peptides. $Ca_v1.2$ localizes to lipid rafts in an insulin-secreting cell line (Xia et al., 2004) and in

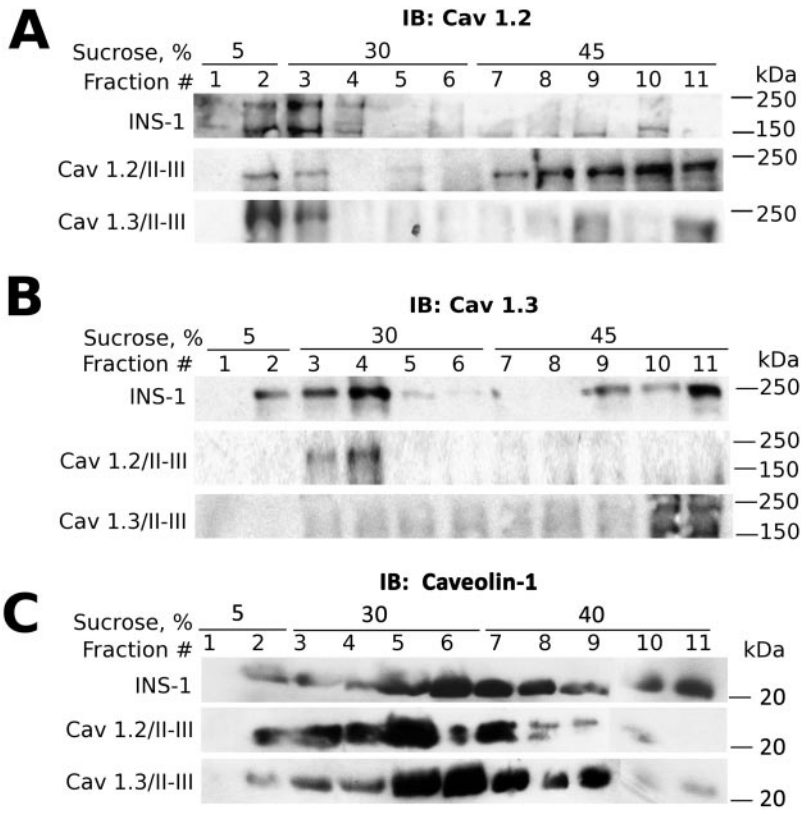

Fig. 5. Displacement of endogenous $Ca_v1.2$ or $Ca_v1.3$ α_1 subunits from detergent-resistant lipid raft membrane fractions by $Ca_v1.2$/II-III or $Ca_v1.3$/II-III peptides. A, Western blot for $Ca_v1.2$ in lysates of INS-1, $Ca_v1.2$/II-II, and $Ca_v1.3$/II-III cells fractionated over discontinuous sucrose gradients. B, Western blot for $Ca_v1.3$ in cell lysates from INS-1, $Ca_v1.2$/II-III, and $Ca_v1.3$/II-III cells fractionated over discontinuous sucrose gradients. C, Western blot for caveolin-1 in cell lysates from INS-1, $Ca_v1.2$/II-III, and $Ca_v1.3$/II-III cells fractionated over discontinuous sucrose gradients. Channel antibodies are directed against the II-III interdomain loop of $Ca_v1.2$ or $Ca_v1.3$. The overexpressed $Ca_v1.2$/II-III (46-kDa) or $Ca_v1.3$/II-III (43-kDa) peptide was detected in all fractions, with a nonuniform distribution that increased from light to dense fractions (data not shown). Each Western blot is representative of at least three independent experiments.

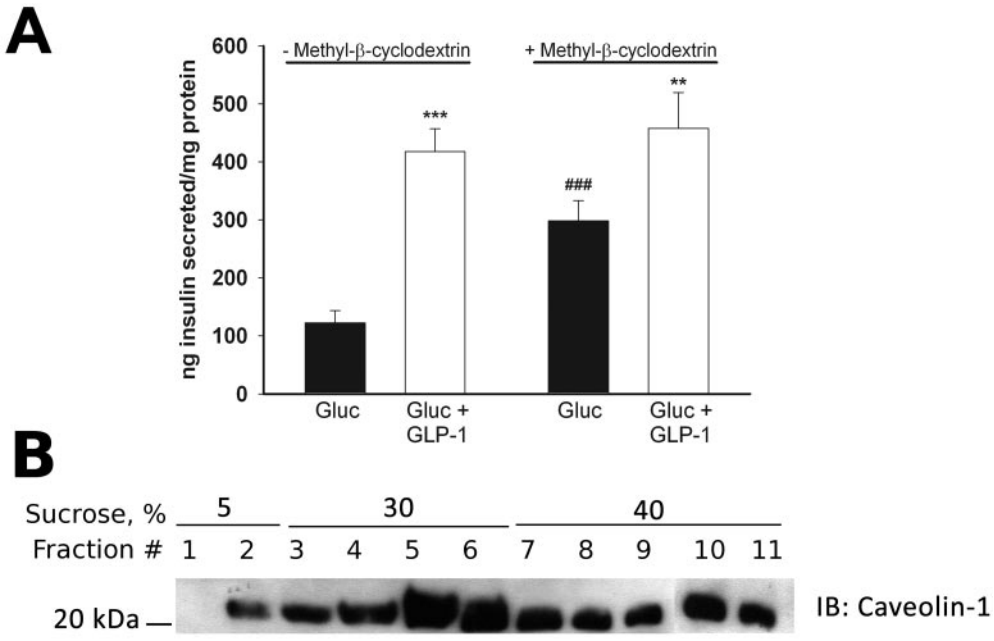

Fig. 6. β-Methyl cyclodextrin enhances GSIS but does not enhance GLP-1 potentiation of GSIS in INS-1 cells. A, insulin secretion in response to 7.5 mM glucose, but not potentiation of GSIS by 50 nM GLP-1, is enhanced by pretreatment of INS-1 cells with the cholesterol binding agent mβCD (10 mM). ***, $P < 0.001$; **, $P < 0.01$ compared with glucose alone; ##, $P < 0.01$ compared with glucose alone in non-mβCD-treated cell ($n = 9$, $F = 19.9$). B, pretreatment of INS-1 cells with 10 mM mβCD does not displace caveolin-1 from the lipid raft fractions of a sucrose density gradient. The Western blot shown is representative of three separate experiments.

cardiac muscle (Balijepalli et al., 2006), but our observation that $Ca_v1.3$ also localizes to lipid rafts in insulin-secreting cells is, to our knowledge, novel. Our results imply that the II-III loops of $Ca_v1.2$ and $Ca_v1.3$ may play a central role in localizing the channels to lipid rafts, possibly through physical interactions with other lipid raft-resident proteins. Thus, binding of the overexpressed II-III loops to their respective partner proteins may competitively inhibit targeting of endogenous L-VGCC to lipid rafts (Fig. 8). The II-III peptide of $Ca_v1.2$ binds directly to the C2a domains of both Piccolo and RIM2 (Shibasaki et al., 2004), two proposed downstream effectors of the cAMP-binding protein EPAC2, a key effector after GLP-1 receptor activation (Kang et al., 2001; Fujimoto et al., 2002; Shibasaki et al., 2007). Piccolo dimerizes with RIM2 in a Ca^{2+}-dependent manner (Fujimoto et al., 2002), and both are implicated in potentiation of GSIS via EPAC2. Knockdown of Piccolo in pancreatic islets with antisense oligonucleotides inhibits cAMP potentiation of GSIS (Fujimoto et al., 2002). Indeed, the II-III loop of $Ca_v1.2$, but not that of $Ca_v1.3$, coimmunoprecipitated full-length, endoge-

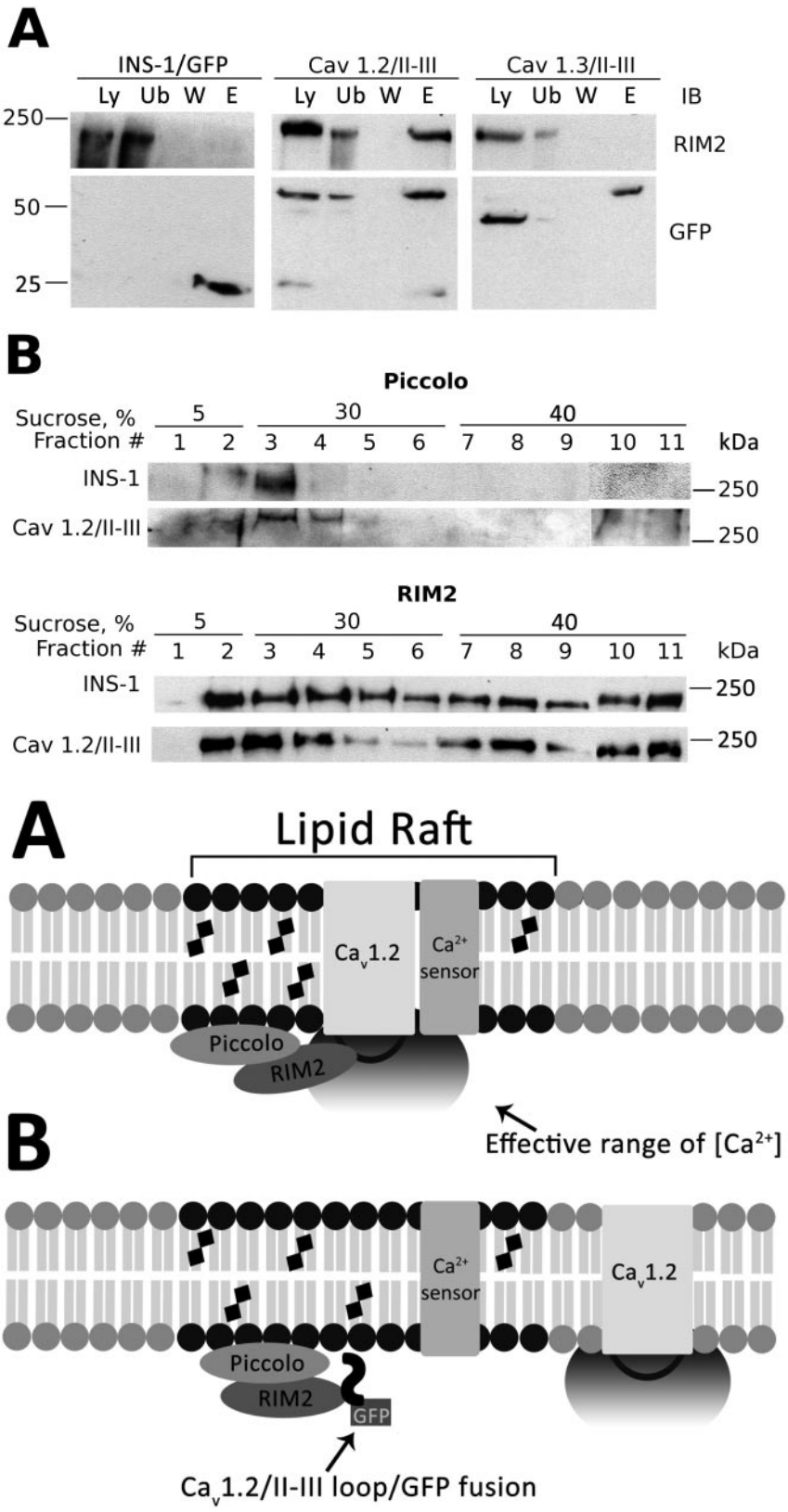

Fig. 7. RIM2 preferentially associates with the $Ca_v1.2$/II-II peptide and is present in lipid rafts. A, RIM2 coimmunoprecipitates with the II-III loop of $Ca_v1.2$. Lysates from INS-1 cells transfected with GFP (INS-1/GFP), $Ca_v1.2$/II-III cells, or $Ca_v1.3$/II-III cells were incubated with agarose beads fused to a GFP antibody. Samples were analyzed by Western blot. Lane Ly represents 50 μg of protein from cell lysates. Lane Ub is the unbound protein after immunoprecipitation. Lane W represents proteins that were removed through a series of washes. The proteins were eluted from the beads using gentle heating in Laemmli buffer (lane E). For lanes 2 to 4 50 μl of each sample was loaded. Blots were also probed with GFP antibody to confirm the location of the II-III loops. Results shown are representative of three independent experiments. B, Western blot of Piccolo and RIM2 from lysates of INS-1 and Cav1.2/II-III cells fractionated over discontinuous sucrose gradients. Each blot is representative of at least three separate experiments.

Fig. 8. Model for inhibition of GLP-1 potentiation of GSIS by displacement of $Ca_v1.2$ or $Ca_v1.3$ from lipid rafts. A, intracellular interdomain II-III loops of $Ca_v1.2$ and 1.3 direct localization of the respective channels to lipid rafts via binding to raft-resident proteins. In $Ca_v1.2$, binding to the raft resident RIM2 anchors the channel in the lipid raft domain. A similar interaction with a yet unidentified protein is proposed to anchor $Ca_v1.3$ to lipid rafts. Other proteins required for insulin exocytosis or extracellular signal-regulated kinase 1/2 phosphorylation are also localized to lipid rafts. B, overexpression of the $Ca_v1.2$/II-III loop/GFP fusion peptide in INS-1 cells competitively displaces the endogenous $Ca_v1.2$ channel from lipid rafts by binding to raft resident protein RIM2, spatially uncoupling them from Ca^{2+}-dependent processes such as GLP-1 potentiation of GSIS. Augmentation of Ca^{2+} influx via the displaced channels with the L-type channel agonist FPL-64176 can partially compensate for the increased distance between channel pore and Ca^{2+}-sensing proteins involved in secretion (see Fig. 1C).

nous RIM2 from INS-1 cells (Fig. 7A). Overexpression of the $Ca_v1.2$/II-III peptide also inhibited potentiation of GSIS by 8-Br-cAMP, whereas overexpression of $Ca_v1.3$/II-III did not. The observation is consistent with the proposed role of RIM2 in EPAC2-mediated cAMP potentiation of GSIS (Shibasaki et al., 2004), and our previous observation that $Ca_v1.2$ couples directly to EPAC2-mediated secretion, whereas $Ca_v1.3$ requires simultaneous activation of PKA to couple to secretion mediated by EPAC2 (Liu et al., 2006).

RIM2 and Piccolo both localized to the Triton X-100-insol-

uble lipid raft fractions on a sucrose density gradient. Interestingly, the localization of RIM2 and Piccolo was not substantially affected by overexpression of the $Ca_v1.2$ II-III loop (Fig. 7B). Our finding that the intracellular II-III loops of $Ca_v1.2$ and 1.3 are critical for lipid raft targeting of the channels parallels a previous study reporting that the intracellular C1 and C2 domains of Ca^{2+}-sensitive AC5 and AC8 are critical determinants of lipid raft targeting for these membrane proteins (Crossthwaite et al., 2005). We propose that RIM2 may act as an anchor that positions $Ca_v1.2$ within a lipid raft domain that serves as an assembly point for effectors of cAMP signaling via EPAC2. However, lipid raft resident proteins that interact with the II-III loop of $Ca_v1.3$, and could potentially serve as anchors for lipid raft localization of $Ca_v1.3$, remain to be identified.

GLP-1 Potentiation of GSIS Requires Specific Localization of $Ca_v1.2$ and $Ca_v1.3$ Channels to Lipid Rafts. Glucose-stimulated insulin secretion (Devis et al., 1975) and its potentiation by GLP-1 are both dependent upon Ca^{2+} influx through L-VGCC (MacDonald et al., 2002). We reported previously that overexpression of the $Ca_v1.3$ II-III peptide, but not the $Ca_v1.2$ II-III peptide, inhibited 11 mM GSIS in INS-1 cells (Liu et al., 2003). Here, we demonstrate overexpression of either the $Ca_v1.2$ or the $Ca_v1.3$ II-III loop markedly suppresses the ability of GLP-1 to potentiate 7.5 mM GSIS in INS-1 cells. The mechanism of this inhibition is not the loss of L-VGCC activity or a shift in activation potential. Interestingly, whole-cell voltage-gated Ba^{2+} current was actually increased by $Ca_v1.2$/II-III peptide overexpression, but the fraction of L-type current was not different from either untransfected INS-1 cells or INS-1 cells overexpressing $Ca_v1.3$/II-III peptide. Our results are consistent with a previous report (Wiser et al., 1999) that acute introduction of the full-length $Ca_v1.2$/II-III peptide into β-cells via patch pipette did not alter ion channel activity but did suppress depolarization-evoked insulin secretion as detected by changes in membrane capacitance. The rescue of GSIS by FPL-64176, a compound that enhances the flux of Ca^{2+} through L-VGCC during membrane depolarization (Zheng et al., 1991) in both $Ca_v1.2$/II-III and $Ca_v1.3$/II-III cells, indicates that L-type channels that are displaced from lipid rafts can effectively couple to GSIS if Ca^{2+} influx is augmented.

Previously, disruption of lipid rafts with methyl-β-cyclodextrin was reported to not affect voltage-gated Ca^{2+} channel activity, but to decrease voltage-gated K^+ current density, and increase glucose-stimulated insulin secretion (Xia et al., 2004). We observed the same stimulation of GSIS, but no difference in GLP-1 potentiation of GSIS, in INS-1 cells treated with methyl-β-cyclodextrin. More recently, chronic inhibition of cholesterol synthesis in MIN6 cells was reported to markedly reduce both GSIS and voltage-gated Ca^{2+} current (Xia et al., 2008). Thus, the effects of overexpression of the $Ca_v1.2$/II-III and $Ca_v1.3$/II-III loops on insulin secretion in INS-1 cells are distinct from those observed using agents that perturb cholesterol concentrations in the plasma membrane or throughout the cell, suggesting that overexpression of the $Ca_v1.2$/II-III or $Ca_v1.3$/II-III loop does not result in general disruption of lipid rafts.

Maximal GLP-1-Stimulated cAMP Accumulation Requires Localization of $Ca_v1.2$ and $Ca_v1.3$ to Lipid Rafts. Primary β-cells predominantly express AC6 (Ca^{2+}-inhibited) and AC8 (Ca^{2+}-stimulated), and INS-1 cells express AC8 (Delmeire et al., 2003). Both of these Ca^{2+}-sensitive adenylyl cyclases are enriched in lipid rafts (Fagan et al., 2000; Smith et al., 2002). Moreover, Ca^{2+} influx via L-VGCC is implicated in the stimulation of Ca^{2+}-dependent adenylyl cyclase (Delmeire et al., 2003). The reduction of GLP-1-stimulated cAMP accumulation in $Ca_v1.2$/II-III and $Ca_v1.3$/II-III cells compared with untransfected INS-1 cells was unexpected. This reduction is not accompanied by attenuation of forskolin responsiveness in either cell line, suggesting that the II-III interdomain peptides do not directly inhibit endogenous adenylyl cyclase activity (Supplemental Fig. 1). Furthermore, the decrease in GLP-1-stimulated cAMP accumulation in $Ca_v1.2$/II-III and $Ca_v1.3$/II-III cells was not rescued by FPL-64176. We propose that localization of L-VGCC to lipid rafts may be essential for maximal stimulation of adenylyl cyclase activity by GLP-1, perhaps as the result of Ca^{2+} influx via L-VGCC potentiating the activity of a Ca^{2+}-activated adenylyl cyclase (i.e., AC8). However, the specific adenylyl cyclase isoforms coupled to GLP-1R-mediated GSIS remain to be identified. A close physical association of L-VGCC with adenylyl cyclase is reported in cardiac myocytes, in which $Ca_v1.2$ and adenylyl cyclases are colocalized to lipid rafts and are coimmunoprecipitated by antibodies to $Ca_v1.2$ along with protein kinase A, β_2-adrenergic receptor, G_s, and protein phosphatase 2a (Balijepalli et al., 2006). Thus, $Ca_v1.2$ is an integral component of a G protein-coupled receptor-mediated signaling complex in cardiac cells, and displacement of the channel from a similar complex with the GLP-1 receptor in INS-1 cells may compromise GLP-1-stimulated cAMP accumulation.

In conclusion, we present evidence that overexpression of the intracellular II-III loop domains of $Ca_v1.2$ and $Ca_v1.3$ can dislodge the corresponding endogenous channels from the lipid raft regions of the membrane in INS-1 cells. For $Ca_v1.2$, the mechanism may involve interaction of the II-III loop domain with the lipid raft resident protein RIM2. The displacement of $Ca_v1.2$ and $Ca_v1.3$ from lipid rafts markedly inhibits GLP-1 potentiation of GSIS in INS-1 cells. It was recently reported that Ca^{2+} secretion coupling was impaired in pancreatic β-cells from the type 2 diabetic Goto Kakizaki rat, despite an increase in voltage-gated Ca^{2+} channel current density (Rose et al., 2007). Thus, it will be of interest to determine whether exclusion of L-VGCC from cholesterol-rich lipid rafts contributes to deficits in GSIS in type 2 diabetes.

References

Asfari M, Janjic D, Meda P, Li G, Halban PA, and Wollheim CB (1992) Establishment of 2-mercaptoethanol-dependent differentiated insulin-secreting cell lines. *Endocrinology* **130:**167–178.

Balijepalli RC, Foell JD, Hall DD, Hell JW, and Kamp TJ (2006) Localization of cardiac L-type Ca(2+) channels to a caveolar macromolecular signaling complex is required for beta(2)-adrenergic regulation. *Proc Natl Acad Sci U S A* **103:**7500–7505.

Bergsten P (2002) Role of oscillations in membrane potential, cytoplasmic Ca2+, and metabolism for plasma insulin oscillations. *Diabetes* **51(Suppl 1):**S171–S176.

Catterall WA (1995) Structure and function of voltage-gated ion channels. *Annu Rev Biochem* **64:**493–531.

Cohen AW, Hnasko R, Schubert W, and Lisanti MP (2004) Role of caveolae and caveolins in health and disease. *Physiol Rev* **84:**1341–1379.

Crossthwaite AJ, Seebacher T, Masada N, Ciruela A, Dufraux K, Schultz JE, and Cooper DM (2005) The cytosolic domains of Ca^{2+}-sensitive adenylyl cyclases dictate their targeting to plasma membrane lipid rafts. *J Biol Chem* **280:**6380–6391.

Cumbay MG and Watts VJ (2001) Heterologous sensitization of recombinant adenylate cyclases by activation of D_2 dopamine receptors. *J Pharmacol Exp Ther* **297:**1201–1209.

Delmeire D, Flamez D, Hinke SA, Cali JJ, Pipeleers D, and Schuit F (2003) Type VIII

adenylyl cyclase in rat beta cells: coincidence signal detector/generator for glucose and GLP-1. *Diabetologia* **46:**1383–1393.
Devis G, Somers G, Van Obberghen E, and Malaisse WJ (1975) Calcium antagonists and islet function. I. Inhibition of insulin release by verapamil. *Diabetes* **24:**247–251.
Fagan KA, Smith KE, and Cooper DM (2000) Regulation of the Ca^{2+}-inhibitable adenylyl cyclase type VI by capacitative Ca^{2+} entry requires localization in cholesterol-rich domains. *J Biol Chem* **275:**26530–26537.
Fujimoto K, Shibasaki T, Yokoi N, Kashima Y, Matsumoto M, Sasaki T, Tajima N, Iwanaga T, and Seino S (2002) Piccolo, a Ca^{2+} sensor in pancreatic beta-cells. Involvement of cAMP-GEFII. Rim2.Piccolo complex in cAMP-dependent exocytosis. *J Biol Chem* **277:**50497–50502.
Griffith IP (1972) The effect of cross-links on the mobility of proteins in dodecyl sulphate-polyacrylamide gels. *Biochem J* **126:**553–560.
Ji J, Yang SN, Huang X, Li X, Sheu L, Diamant N, Berggren PO, and Gaisano HY (2002) Modulation of L-type Ca2+ channels by distinct domains within snap-25. *Diabetes* **51:**1425–1436.
Kang G, Chepurny OG, and Holz GG (2001) cAMP-regulated guanine nucleotide exchange factor II (Epac2) mediates Ca2+-induced Ca2+ release in INS-1 pancreatic beta-cells. *J Physiol* **536:**375–385.
Leung YM, Kwan EP, Ng B, Kang Y, and Gaisano HY (2007) SNAREing voltage-gated K+ and ATP-sensitive K+ channels: tuning beta-cell excitability with syntaxin-1A and other exocytotic proteins. *Endocr Rev* **28:**653–663.
Liu G, Dilmac N, Hilliard N, and Hockerman GH (2003) Ca(v)1.3 is preferentially coupled to glucose-stimulated insulin secretion in the pancreatic beta-cell line INS-1. *J Pharmacol Exp Ther* **305:**271–278.
Liu G, Hilliard N, and Hockerman GH (2004) Cav1.3 is preferentially coupled to glucose-induced $[Ca^{2+}]_i$ oscillations in the pancreatic beta cell line INS-1. *Mol Pharmacol* **65:**1269–1277.
Liu G, Jacobo SM, Hilliard N, and Hockerman GH (2006) Differential modulation of Cav1.2 and Cav1.3-mediated glucose-stimulated insulin secretion by cAMP in INS-1 cells: distinct roles for exchange protein directly activated by cAMP 2 (Epac2) and protein kinase A. *J Pharmacol Exp Ther* **318:**152–160.
MacDonald PE, El-Kholy W, Riedel MJ, Salapatek AM, Light PE, and Wheeler MB (2002) The multiple actions of GLP-1 on the process of glucose-stimulated insulin secretion. *Diabetes* **51** (**Suppl 3):**S434–S442.
Rajan AS, Aguilar-Bryan L, Nelson DA, Yaney GC, Hsu WH, Kunze DL, and Boyd AE 3rd (1990) Ion channels and insulin secretion. *Diabetes Care* **13:**340–363.
Rose T, Efendic S, and Rupnik M (2007) Ca^{2+}-secretion coupling is impaired in diabetic Goto Kakizaki rats. *J Gen Physiol* **129:**493–508.
Shibasaki T, Sunaga Y, Fujimoto K, Kashima Y, and Seino S (2004) Interaction of ATP sensor, cAMP sensor, Ca^{2+} sensor, and voltage-dependent Ca^{2+} channel in insulin granule exocytosis. *J Biol Chem* **279:**7956–7961.
Shibasaki T, Takahashi H, Miki T, Sunaga Y, Matsumura K, Yamanaka M, Zhang C, Tamamoto A, Satoh T, Miyazaki J, et al. (2007) Essential role of Epac2/Rap1 signaling in regulation of insulin granule dynamics by cAMP. *Proc Natl Acad Sci U S A* **104:**19333–19338.
Smith KE, Gu C, Fagan KA, Hu B, and Cooper DM (2002) Residence of adenylyl cyclase type 8 in caveolae is necessary but not sufficient for regulation by capacitative Ca(2+) entry. *J Biol Chem* **277:**6025–6031.
Song H, Nie L, Rodriguez-Contreras A, Sheng ZH, and Yamoah EN (2003) Functional interaction of auxiliary subunits and synaptic proteins with Ca(v)1.3 may impart hair cell Ca2+ current properties. *J Neurophysiol* **89:**1143–1149.
Syme CA, Zhang L, and Bisello A (2006) Caveolin-1 regulates cellular trafficking and function of the glucagon-like peptide 1 receptor. *Mol Endocrinol* **20:**3400–3411.
Tsujikawa H, Song Y, Watanabe M, Masumiya H, Gupte SA, Ochi R, and Okada T (2008) Cholesterol depletion modulates basal L-type Ca2+ current and abolishes its adrenergic enhancement in ventricular myocytes. *Am J Physiol Heart Circ Physiol* **294:**H285–H292.
Wiser O, Trus M, Hernandez A, Renstrom E, Barg S, Rorsman P, and Atlas D (1999) The voltage sensitive lc-type Ca2+ channel is functionally coupled to the exocytotic machinery. *Proc Natl Acad Sci U S A* **96:**248–253.
Wollheim CB and Sharp GW (1981) Regulation of insulin release by calcium. *Physiol Rev* **61:**914–973.
Xia F, Gao X, Kwan E, Lam PP, Chan L, Sy K, Sheu L, Wheeler MB, Gaisano HY, and Tsushima RG (2004) Disruption of pancreatic β-cell lipid rafts modifies Kv2.1 channel gating and insulin exocytosis. *J Biol Chem* **279:**24685–24691.
Xia F, Xie L, Mihic A, Gao X, Chen Y, Gaisano HY, and Tsushima RG (2008) Inhibition of cholesterol biosynthesis impairs insulin secretion and voltage-gated calcium channel function in pancreatic beta-cells. *Endocrinology* **149:**5136–5145.
Yang SN, Larsson O, Bränström R, Bertorello AM, Leibiger B, Leibiger IB, Moede T, Köhler M, Meister B, and Berggren PO (1999) Syntaxin 1 interacts with the L(D) subtype of voltage-gated Ca(2+) channels in pancreatic beta cells. *Proc Natl Acad Sci U S A* **96:**10164–10169.
Zheng W, Rampe D, and Triggle DJ (1991) Pharmacological, radioligand binding, and electrophysiological characteristics of FPL 64176, a novel nondihydropyridine Ca^{2+} channel activator, in cardiac and vascular preparations. *Mol Pharmacol* **40:**734–741.

Address correspondence to: Dr. Gregory H. Hockerman, 575 Stadium Mall Dr., West Lafayette, IN 47907-2091. E-mail: gregh@pharmacy.purdue.edu